ACS APPLIED MATERIALS & INTERFACES

Research Article

www.acsami.org

Oxygen Reduction Electrocatalyst of Pt on Au Nanoparticles through Spontaneous Deposition

Yu Dai[†,‡] and Shengli Chen*[,‡]

[†]Faculty of Material Science and Chemistry, China University of Geosciences, Wuhan 430074, China

[‡]Hubei Electrochemical Power Sources Key Laboratory, Department of Chemistry, Wuhan University, Wuhan 430072, China

ABSTRACT: A straightforward one-step spontaneous deposition approach for growth of Pt atomic shell on Au nanoparticles and the superior activity and durability of the resulted Pt-on-Au nanoparticles for the oxygen reduction reaction (ORR) are reported. Transmission electron microscopy, X-ray photoelectron spectroscopy, energy-dispersive spectrometry, and electrochemical measurements indicate that Pt can be spontaneously deposited on Au surface upon simply dispersing carbon-supported Au nanoparticles in $PtCl_4^{2-}$-containing solution, without introducing any extraneous reducing agents or any pre/post-treatments. The deposited Pt atoms are uniformly distributed on the surface of Au nanoparticles, with coverage tunable by the concentration of $PtCl_4^{2-}$ and temperatures. An approximate monolayer of Pt forms at temperature of ca. 80 °C and $PtCl_4^{2-}$ concentrations of above 10^{-4} mol/L. The obtained Pt-on-Au core−shell nanoparticles catalyze the ORR with specific and mass activities of Pt that are 3.5 times higher than that of pure Pt nanoparticles. Moreover, they exhibit no visible activity degradation after undergoing long-term oxidization/reduction cycling in O_2-saturated acid media, therefore showing great prospect as durable cathode electrocatalysts in proton-exchange membrane fuel cells.

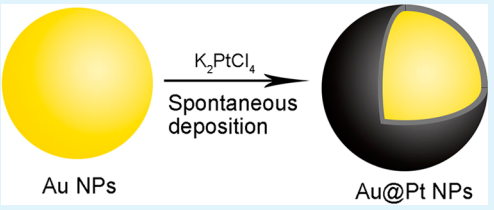

KEYWORDS: *oxygen reduction reaction, low-platinum electrocatalyst, core−shell structure, gold, spontaneous deposition*

1. INTRODUCTION

Currently, proton-exchange membrane fuel cells (PEMFCs) have a considerably high demand of the scarce Pt in their cathodes, due to the relatively sluggish kinetics of the oxygen reduction reaction (ORR), even on Pt,[1] and the unsatisfying durability of current Pt nanoparticle catalysts under the oxidizing and acidic conditions in cathodes of PEMFCs when used as transportation powers.[2] This has been a severe obstacle to the widespread application of the PEMFCs. Deposition of Pt on nanoparticles of relatively abundant metals is among the most efficient strategies to save Pt in catalysts. Moreover, surface Pt atoms deposited on properly chosen core metals could have enhanced intrinsic catalytic activity over those on the pure Pt surface, due to the so-called strain and ligand effects.[3] A variety of transition metals, such as Fe, Co Ni, Cu, Y, etc., have been shown to significantly promote the ORR activity of Pt when acting as core metals. The resultant electrocatalysts, however, could have durability problem in long-term use due to most of the transition metals suffering from acid leaching.

In comparison with Pt, Au is considerably more abundant in nature. Besides, Au is among the most stable metals that are resistant to the oxidative corrosion in acidic media. Recently, Shao et al.[4] have shown that the electrocatalyst of Pt deposited on Au nanoparticles exhibited remarkably enhanced activity for the ORR as compared with the pure Pt nanoparticles. Therefore, Au should be greatly advantageous as core material for constructing surface-only Pt electrocatalysts for the ORR. Nanoparticulate catalysts of Pt on Au may be fabricated through chemical reduction deposition[5,6] and redox-displacement of underpotential-deposited (UPD) Cu monolayers.[4,7] These methods usually require careful experimental control to avoid formation of Pt islands and/or dendritic branches instead of uniform Pt shells. Redox displacement of UPD Cu monolayers is so far the most effective approach for Pt monolayer deposition on other noble metals. However, this two-step deposition approach is somewhat cumbersome and may suffer from overdeposition of Cu and oxidation of Cu monolayer in the subsequent electrode transfer and Cu displacement processes.[8] As well, this two-step method may have a limitation in scale-up catalyst production, since the UPD Cu preparation must be carried out electrochemically by loading the core nanoparticles on a substrate electrode.

Spontaneous deposition, that is, deposition of metals upon bringing a substrate into contact with solution containing ionic metal species without introducing any extraneous reducing agents,[9] should be among the most straightforward approaches for scalable catalyst preparation. There are considerable recent works that report the fabrication of Pt on Au catalysts through the so-called spontaneous deposition processes.[10−16] Strictly speaking, however, the formation of Pt in most of these works was not simply through spontaneous deposition, because a pre- or post-treatment step was involved in addition to a spontaneous step. Therefore, they are still two-step deposition methods. In some of these works, a pretreatment of Au substrate materials, for example, soaking in $NaBH_4$ solution[10] or electrochemical polarization at a negative potential,[10−12] was

Received: October 21, 2014
Accepted: December 16, 2014
Published: December 16, 2014

DOI: 10.1021/am5073029
ACS Appl. Mater. Interfaces 2015, 7, 823−829

Table 1. Compositions of $AuPt_x$/C Samples Obtained by Immersing Au/C in Solutions Containing $PtCl_4^{2-}$ of Different Concentrations (c) under Different Temperatures (T)

c (mol/L)	1×10^{-2}		6×10^{-4}				1×10^{-5}	
T (°C)	80	30	80	50	30	25	80	30
$AuPt_x$ composition	$AuPt_{0.58}$	$AuPt_{0.29}$	$AuPt_{0.58}$	$AuPt_{0.38}$	$AuPt_{0.29}$	$AuPt_{0.20}$	$AuPt_{0.04}$	$AuPt_{0.04}$

employed to form chemisorbed hydrogen atoms (H), following which Pt spontaneous deposition was realized upon immersing the treated materials in solutions containing ionic Pt species. This type of Pt deposition method is similar to the UPD Cu displacement. In some other works, it was shown that Pt precursor species, for example, Pt complex[13−15] and/or $Pt(OH)_2$,[16] can spontaneously adsorb/form on Au substrate surface when immersed in solution containing ionic Pt species; subsequent electrochemical treatment at negative potential would result in Pt deposition on Au.

One-step spontaneous deposition without involving any pre- and/or post-treatment steps would be highly expected. This has been demonstrated for Pt deposition on single-crystal and nanoparticulate Ru.[17−19] It was proposed that Pt spontaneous deposition is a result of two coupling half-cell reactions at the Ru surface, namely, the water dissociation (e.g., $Ru^0 + x(H_2O) \rightarrow RuO_xH_y + (2x - y)H^+ + (2x - y)e^-$) and the reduction of Pt species (e.g., $PtCl_6^{2-}+4e^- \rightarrow Pt^0+6Cl^-$), which constitute a galvanic cell. The galvanic cell deposition mechanism was supported by the fact that the spontaneous deposition occurred only on oxide-free Ru surface.[19] In this study, we show that one-step spontaneous deposition of Pt can also take place on carbon-supported Au nanoparticles (Au/C) in $PtCl_4^{2-}$ solution. Moreover, it is found that the coverage of Pt spontaneously deposited on Au nanoparticle surface crucially depends on the temperatures and $PtCl_4^{2-}$ concentrations. Using the spontaneous deposition, we obtained carbon-supported Pt-on-Au nanoparticles with a series of Pt/Au atomic ratios ($AuPt_x$/C), which exhibit promising activity and durability as ORR electrocatalysts.

2. EXPERIMENTAL SECTION

2.1. Materials Preparation. *2.1.1. Au/C.* Au colloidal solution was prepared by adding 0.03 g of sodium boron hydride to an 800 mL solution containing 1.57 mL of chloroauric acid (0.04 g/mL) and 0.08 g of sodium citrate. Au nanoparticles were then loaded on the surface of XC-72R carbon black by adding 0.12 g of XC-72R into the prepared Au colloidal solution. The loading process lasted for ca. 48 h under vigorous stirring at room temperature. Au/C was collected by repeated centrifugation and washing and was then dried in vacuum overnight. Inductively coupled plasma (ICP) results indicated that the actual loading of Au on the carbon support was 17.4 ± 0.5 wt %.

2.1.2. $AuPt_x$/C. To prepare $AuPt_x$/C, the Au/C obtained above was first ultrasonically dispersed in water (2 mg/mL), and the suspension was then heated to the desired temperature, following which the required amount of K_2PtCl_4 was added into the suspension to allow spontaneous deposition of Pt on Au at the constant temperature for ~3 h under vigorous stirring. $AuPt_x$/C was collected by repeated centrifugation and washing with water several times and then dried in vacuum overnight at room temperature. As will be shown, ICP results indicated the amounts of Pt deposited on Au depend on the temperatures and concentrations of $PtCl_4^{2-}$. Deposition temperatures of 25, 30, 50, and 80 °C and K_2PtCl_4 concentrations of 10^{-5}, 10^{-4}, 6×10^{-4}, and 10^{-2} mol/L were used.

2.2. Materials Characterization. Transmission electron microscopy (TEM) images were obtained on a JEOL JEM-2010F transmission electron microscope. The inductively coupled plasma atomic emission spectroscopy (ICP-AES) was performed on an IRIS Intrepid II XSP from Thermo Electron Corporation. X-ray fluorescence (XRF) analysis was determined by a Shimadzu EDX-720 energy dispersive X-ray fluorescence spectrometer with Si as detector and liquid nitrogen as cryogen. Powder X-ray diffraction (XRD) patterns of various catalysts were obtained on a Shimadzu XRD-6000 X-ray diffractometer using a Cu KR radiation source operating at 40 kV and 30 mA. Angle-resolved X-ray photoelectron spectroscopy (XPS) measurements were carried out using a Kratos Ltd. XSAM-800 spectrometer with Cu Kα radiator. The data were fitted using the software XPSPEAK41 (Shirley function as baseline, Gauss-Lorentzian linearity fitting).

Electrochemical measurements were performed with a three-electrode configuration. The working electrodes were the commonly used thin-film rotating-disk-electrode (RDE) made by coating the studying catalysts as a thin film onto a glass carbon (GC) RDE substrate (diameter: 5 mm) with Nafion ionomer as the binding agent. Briefly, 5 mg of catalyst sample was dispersed ultrasonically in 1 mL of solution of Nafion ionomer in isopropyl alcohol (0.05 wt %). An aliquot (6 μL) of the resulting suspension was then pipetted onto GC RDE to form a thin catalyst film. The total loading of catalyst sample (metal + carbon) on GC electrode was ca. 153 $\mu g/cm^2$. The counter electrode was a Pt foil, and the reference electrode was a saturated calomel electrode (SCE), which was separated from the working electrode by a Luggin capillary. However, all the potentials were expressed on the scale of the reversible hydrogen electrode (RHE) in this paper. The working electrolyte solution was 0.1 M $HClO_4$ aqueous solution.

3. RESULTS AND DISCUSSION

3.1. Spontaneous Deposition of Pt on Au/C: Effects of Temperature and $PtCl_4^{2-}$ Concentration. XRF, ICP, and XPS were used to determine the compositions of the obtained catalyst samples. According to the ICP data, the content of Au in Au/C samples was 17.4 ± 0.5 wt %. For each $AuPt_x$/C sample, XRF and ICP data gave very similar Pt/Au atomic ratios. In the following, only the ICP results are used. As shown in Table 1, the compositions of the obtained $AuPt_x$/C samples vary with deposition temperature (T) and $PtCl_4^{2-}$ concentration (c). As the concentration of $PtCl_4^{2-}$ was ca. 10^{-5} mol/L, the content of Pt spontaneously deposited on Au was very low, regardless of deposition temperatures. Upon increasing the $PtCl_4^{2-}$ concentration to above 10^{-4} mol/L, considerable amounts of Pt can be spontaneously deposited on Au nanoparticles. As the $PtCl_4^{2-}$ concentration was increased to above 6×10^{-4} mol/L, further increase hardly changed the amount of Pt deposition. Increase in the deposition temperature, however, can significantly enhance the spontaneous deposition of Pt on Au. At temperature of 80 °C, Pt/Au atomic ratio up to ca. 0.58 can be reached through the spontaneous deposition process.

Figure 1 shows angle-resolved XPS spectra for $AuPt_x$/C samples of different Pt/Au atomic ratios in binding energy range of 4f orbitals of Pt and Au. For comparison, the Pt_{4f} XPS spectra for the commercial 20 wt % Pt/C sample from Johnson-Matthey (JM) is also given. The metal particles in the JM 20 wt % Pt/C catalysts are typically sized ~3.2 nm with a narrow size distribution. One can find that the areas under Pt_{4f} spectra of various samples increase with the Pt/Au atomic ratios. By correcting the XPS sensitivities of Pt and Au, areas

DOI: 10.1021/am5073029
ACS Appl. Mater. Interfaces 2015, 7, 823−829

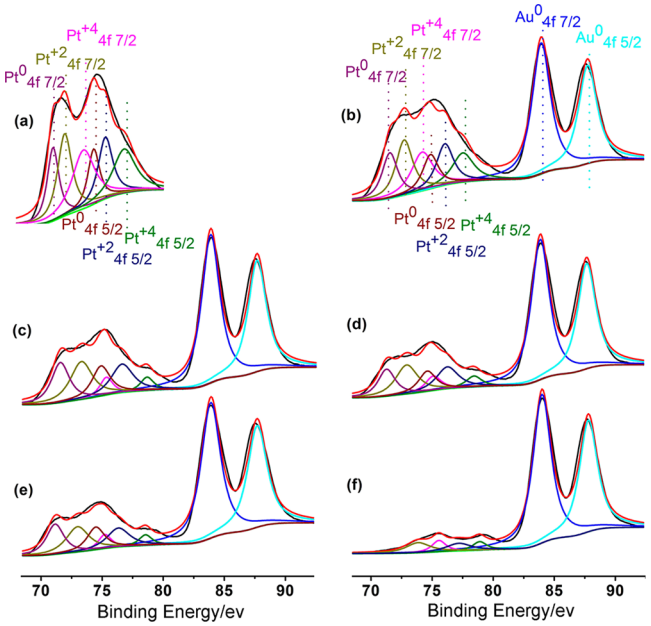

Figure 1. XPS results for (a) Pt/C, (b) $AuPt_{0.58}$, (c) $AuPt_{0.38}$, (d) $AuPt_{0.29}$, (e) $AuPt_{0.20}$, and (f) $AuPt_{0.04}$. Black solid lines: measured XPS spectra; red solid lines: superposition of deconvoluted component spectra; green solid lines: background responses.

under Pt_{4f} and Au_{4f} spectra gave Pt/Au atom ratios of 1.13:1, 0.72:1, 0.57:1, and 0.53:1, respectively, for samples of $AuPt_{0.58}$/C, $AuPt_{0.38}$/C, $AuPt_{0.29}$/C, and $AuPt_{0.20}$/C, which were ~2 times of those given by ICP. This meant that Pt stays on the surface of Au in various $AuPt_x$/C samples, because XPS responses are sensitive only to the compositions in the near-surface region of a sample.

Deconvolution of the measured XPS spectra through Gauss–Lorentzian fitting can give the distribution of valence states of Au and Pt atoms in the near-surface region. It can be seen that the near-surface Au atoms in $AuPt_x$/C samples are predominantly in nonoxidized state, while Pt_{4f} spectra were constituted of responses of Pt(IV) and Pt(II) as well as Pt(0) states. The XPS responses of Pt(IV) and Pt(II) states should not be an evidence for the presence of the adsorbed ionic Pt species such as $PtCl_4^{2-}$ on Au surface or carbon support because these XPS responses are also seen for the commercial Pt/C sample (Figure 1a). It seems to be a common phenomenon for Pt-based nanoparticle catalysts to exhibit XPS responses of oxidation states of Pt, which is most probably a result of the oxidation of surface Pt atoms in air. Because Au is more inert to oxidation than Pt, no obvious XPS responses of Au oxidation states were seen for $AuPt_x$/C samples. In addition, Pt on the surfaces of these samples would also protect Au from oxidation.

Table 2 shows the relative compositions of Pt(IV), Pt(II), and Pt(0) states in different Pt-containing samples. The ratios of Pt(IV) and Pt(II) states over Pt(0) for various $AuPt_x$/C samples are even lower than that for the commercial Pt/C, which suggests that the surface Pt atoms in the $AuPt_x$/C samples are somewhat less oxophilic than those in the Pt/C. This is possibly because the metal nanoparticles in the commercial Pt/C sample have smaller sizes.

To further exclude the presence of adsorbed $PtCl_4^{2-}$ in the prepared $AuPt_x$/C samples, we added ammonia into the dispersion of the $AuPt_x$/C samples followed by addition of silver nitrate. If there were adsorbed $PtCl_4^{2-}$ species in the prepared $AuPt_x$/C samples, the chloride ions in $PtCl_4^{2-}$ would be substituted by ammonia and then react with Ag^+ to form AgCl. However, no precipitation was observed in these experiments. Therefore, we may conclude that the Pt species in $AuPt_x$/C samples are not the adsorbed $PtCl_4^{2-}$.

Spontaneous deposition of Pt on Au nanoparticles was also evidenced by TEM characterization results. In Figure 2, TEM images and corresponding particle size distribution histograms of Au/C, $AuPt_{0.29}$/C, and $AuPt_{0.58}$/C samples are compared. The average sizes of metal particles in $AuPt_{0.29}$/C and $AuPt_{0.58}$/C samples were ca. 3.70 and 4.04 nm, respectively, which were larger than the sizes of Au particles (ca. 3.45 nm) in original Au/C samples. The average distance between nearest neighbor atomic rows, obtained from high-resolution TEM images of ~50 particles in each sample, was found to be obviously shorter in the outer region than that in the inner region (~0.228 vs ~0.236 nm in $AuPt_{0.29}$ and $AuPt_{0.58}$ particles), which suggested a Au–Pt core–shell structure of particles in these samples.

To further verify the Pt-on-Au structure, EDS spectra of $AuPt_{0.58}$ nanoparticles were sampled with scanning TEM mode along with dark field images. The results are given in Figure 3, which shows that Pt and Au were distributed approximately in the same area on carbon support. From the overlay graph of EDS scanning spectra of Au and Pt, one can find that the image area of Pt is larger than that of Au, indicating that Pt locates in the outer region of particles.

Figure 4 compares XRD spectra of the Pt/C, Au/C, and $AuPt_x$/C samples of different x. The $AuPt_x$/C samples exhibited diffraction peaks nearly identical to those for Au/C. This suggested that Pt formed thin shell on Au particle surface rather than islands of multiple layers; otherwise, one would observe XRD peaks for $AuPt_x$/C samples at 2θ values close to those exhibited by Pt/C. Assuming that Au nanoparticles have cuboctahedral shapes, deposition of a Pt monolayer shell on ca. 3.5 nm Au particles would lead to an approximate composition of $AuPt_{0.5}$, and the particle size would increase to ca. 4 nm. Thus, $AuPt_{0.58}$ in principle should possess a monolayer shell of Pt on Au if Pt undergoes two-dimensional (2-D) epitaxial deposition. The average particle size of 4.04 nm for $AuPt_{0.58}$ indicated by TEM images seemed to suggest an approximate monolayer Pt on this sample. As seen from TEM images in Figure 2, $AuPt_x$ nanoparticles had relatively smooth surface, with no visible islands or dendritic branches.

The exact mechanism of the spontaneous Pt deposition on Au nanoparticle surfaces shown above is not yet clear. Considering that the water dissociation on Au surface occurs at considerably positive potentials, the galvanic cell mechanism proposed for Pt deposition on Ru surface[19] might not apply to the present case of Pt deposition on Au. It seems also unlikely that the deposited Pt atoms have displaced surface Au atoms

Table 2. Relative Compositions of Pt(IV), Pt(II), and Pt(0) States, Given in the Form of Pt(IV): Pt(II): Pt(0), in $AuPt_x$/C and Pt/C Samples Obtained from Fitted XPS Peak Areas

$AuPt_{0.58}$/C	$AuPt_{0.38}$/C	$AuPt_{0.29}$/C	$AuPt_{0.20}$/C	$AuPt_{0.04}$/C	Pt/C
1.17:1.30:1	0.31:1.15:1	0.48:1.36:1	0.34:1.07:1	0.92:1.16:1	1.53:1.37:1

DOI: 10.1021/am5073029
ACS Appl. Mater. Interfaces 2015, 7, 823–829

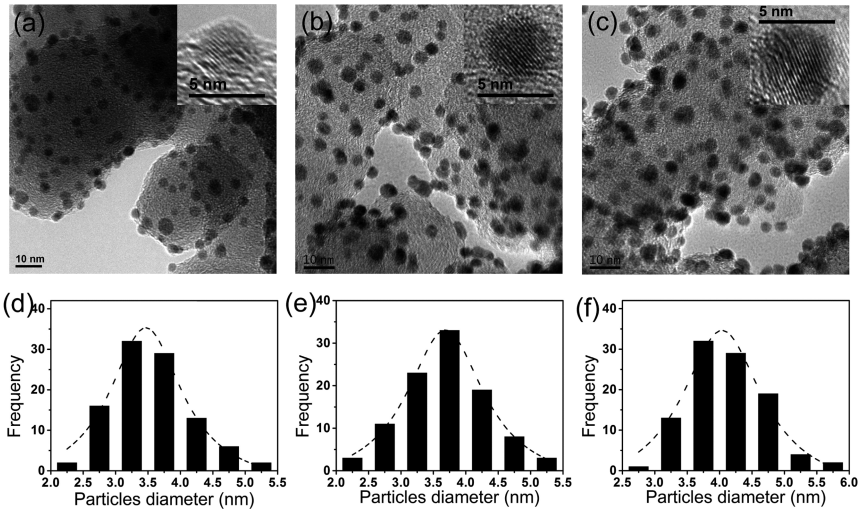

Figure 2. TEM images and corresponding particle size distribution histograms for (a, d) Au/C, (b, e) $AuPt_{0.29}$, and (c, f) $AuPt_{0.58}$ samples. (inset) In each TEM image is the representative high-resolution image of a single particle.

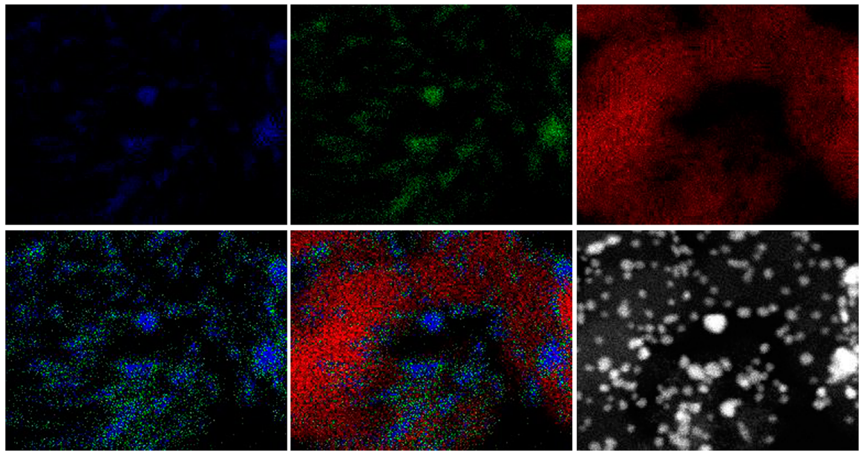

Figure 3. EDS spectra of the dark field image and surface scanning in the STEM mode of $AuPt_{0.58}$ (blue: Au, green: Pt, red: C).

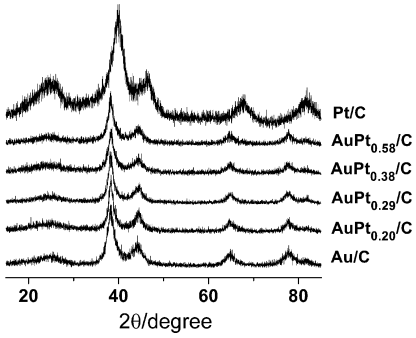

Figure 4. XRD spectra of Pt/C, Au/C, and $AuPt_x/C$.

since the $AuCl_4^-/Au$ redox couple has more positive standard redox potential than that of $PtCl_4^{2-}/Pt$ couple. We measured the concentrations of soluble Au species in the suspensions after the spontaneous Pt deposition. The obtained values were similarly infinitesimal relative to those obtained in suspension containing only Au/C and were very much smaller than those expected for the displaced Au atoms by the deposited Pt.

Although the $AuCl_4^-/Au$ redox couple has more positive standard redox potential than that of $PtCl_4^-/Pt$ couple, the real equilibrium potential of the $AuCl_4^-/Au$ couple in the initial suspension could be more negative than that of the $PtCl_4^{2-}/Pt$ because the initial concentration of soluble Au species in the suspension and the coverage of Pt on the surface of Au particles were nearly zero. Therefore, it is likely that a trace amount of Pt atoms can be deposited on Au nanoparticle surface upon dispersing carbon-supported Au nanoparticles in $PtCl_4^{2-}$-containing solution, especially at the Au surface atoms with low coordination number. The resulting Pt atoms may have the ability to catalyze the further reduction of $PtCl_4^{2-}$ on the Au nanoparticle surface. For example, it is possible that the reduction of $PtCl_4^{2-}$ and the oxidation of water on newly formed Pt atoms form galvanic cells, which lead to deposition of Pt around the formed Pt atoms. Further elaborate studies are necessary to unveil the mechanism of the spontaneous Pt deposition on Au nanoparticles.

3.2. Electrocatalytic Properties of Surface Pt Spontaneously Deposited on Au/C. By loading samples of various carbon-supported metal nanoparticles, namely, Au/C, $AuPt_x/C$ of different x, and Pt/C, on GC RDE (see Experimental Section for details), their electrocatalytic properties were compared. Figure 5 shows the cyclic voltammograms recorded in different potential regions in argon-saturated 0.1 mol/L $HClO_4$. The $AuPt_{0.04}/C$ exhibited very similar voltammetric responses to those of Au/C, only showing features associated

DOI: 10.1021/am5073029
ACS Appl. Mater. Interfaces 2015, 7, 823−829

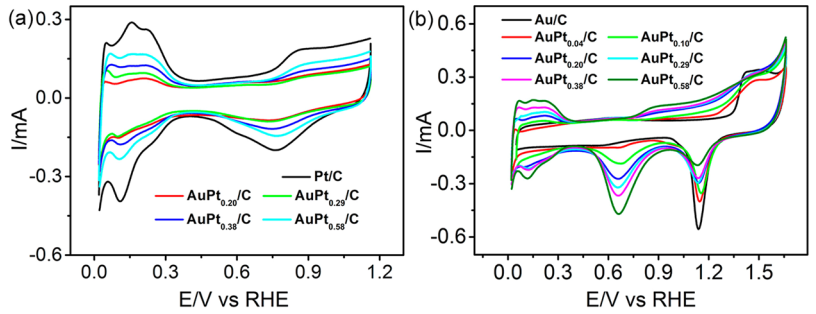

Figure 5. CVs of Au/C, $AuPt_x/C$, and Pt/C samples recorded in potential ranges of (a) 0.05−1.2 V and (b) 0.05−1.7 V, respectively. Potential scanning rate: 50 mV/s.

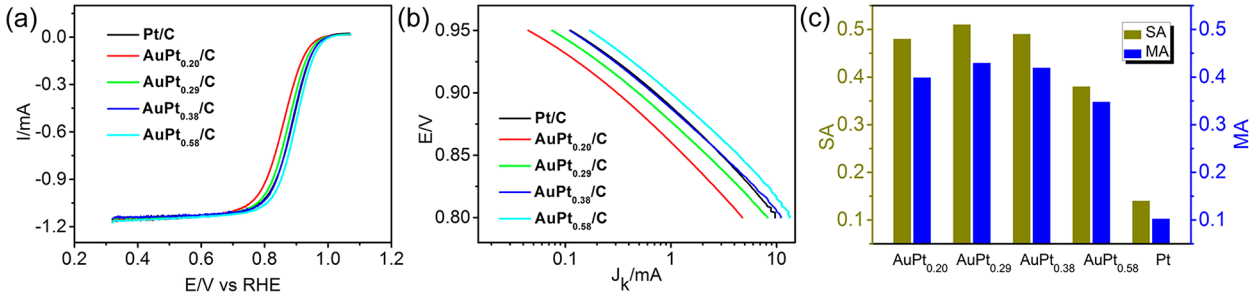

Figure 6. (a) Steady-state polarization curves obtained with linear potential scan (5 mV/s) at electrode rotation rate of 1600 rpm in O_2-saturated 0.1 M $HClO_4$ and (b) mass-transport corrected Tafel curves for the ORR on electrodes loaded with Pt/C and $AuPt_x/C$ samples (153 $\mu g/cm^2$). (c) Specific and mass activity of Pt for different samples at 0.9 V.

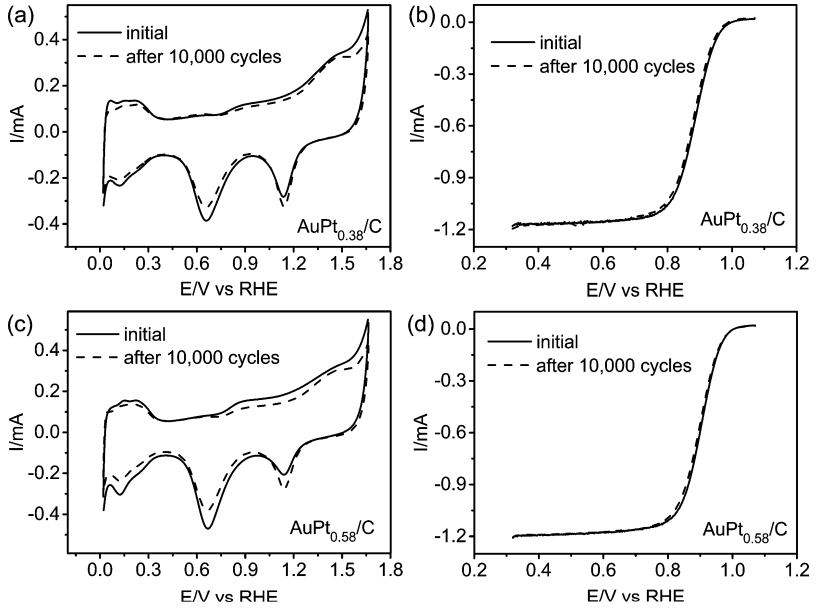

Figure 7. (a, c) Cyclic voltammograms and (b, d) ORR polarization curves of $AuPt_{0.38}/C$ and $AuPt_{0.58}/C$ catalyst sample before and after accelerated electrochemical degradation tests of 10 000 cycles of potential cycling between 0.6 and 1.1 V with potential scanning rate of 50 mV/s in 0.1 M $HClO_4$ saturated with O_2.

with the surface oxidation and reduction of Au (oxidation peak above 1.2 V and reduction peak between 1.0 and 1.3 V), while the voltammetric responses of Pt, for example, reductive and oxidative peaks for hydrogen adsorption/desorption in potential region between 0.05 and 0.4 V and reduction peak for removal of Pt surface oxides in potential region between 1.0 and 0.5 V, were hardly seen. For $AuPt_x/C$ samples with larger x (prepared in solutions with $PtCl_4^{2-}$ concentrations higher than 10^{-4} mol/L), voltammetric features of Pt were clearly seen. Although CV features of Pt became increasingly obvious, and those of Au were largely depressed with increase of x for $AuPt_x/C$ samples, the voltammetric peak associated with the reduction of Au oxide remained visible for $AuPt_{0.58}/C$, which, as discussed earlier, in principle should possess a monolayer Pt shell. This suggested that Pt did not undergo ideal 2-D epitaxial growth on Au surface in spontaneous deposition process, so that small amounts of Au remained uncovered by Pt.

DOI: 10.1021/am5073029
ACS Appl. Mater. Interfaces 2015, 7, 823−829

Figure 6 compares the electrocatalytic activity of $AuPt_x/C$ and Pt/C samples. The steady-state polarization curves (Figure 6a) were obtained with linear potential scan (5 mV/s) at electrode rotation rate of 1600 rpm in O_2-saturated 0.1 M $HClO_4$. Since the sample loading (metal + carbon) on electrode was the same for different samples (ca. 153 $\mu g/cm^2$), the Pt content on electrode was 5.1, 7.3, 9.3, 13.9, and 30.6 $\mu g/cm^2$ for $AuPt_{0.20}/C$, $AuPt_{0.29}/C$, $AuPt_{0.38}/C$, $AuPt_{0.58}/C$, and Pt/C, respectively. It can be seen that the ORR polarization curve approaches that of Pt/C as x is larger than 0.3 in $AuPt_x/C$. For $AuPt_{0.58}/C$, the polarization curve showed more positive onset and half-wave potentials (low overpotentials) than Pt/C, despite the Pt content on $AuPt_{0.58}/C$ electrode was considerably lower than that of Pt/C (13.9 vs 30.6 $\mu g/cm^2$). This implied that $AuPt_{0.58}/C$ had higher Pt mass activity for the ORR than Pt/C.

On the basis of the polarization curves in Figure 6a, we can have Tafel plots of the mass-transport corrected current (kinetic current) for the ORR as a function of electrode potential, which are shown in Figure 6b. The kinetic currents in Figure 6b are normalized, respectively, by the mass and electrochemical surface area (ECSA) of Pt on each electrode, thus giving the so-called mass activity (MA) and specific activity (SA) of Pt for the ORR. The ECSA of Pt for each sample can be obtained by the charge involved in the hydrogen adsorption/desorption peaks in CV (Figure 5a). It can be seen that $AuPt_x/C$ samples gave very similar Tafel slopes to those of Pt/C, which indicated that $AuPt_x/C$ and Pt/C possessed the similar ORR reaction pathway. In addition, various $AuPt_x/C$ samples exhibited very similar MA and SA of Pt. Figure 6c compares the MA and SA for various sample catalysts at 0.9 V. In comparison with Pt/C, the SA and MA of Pt in $AuPt_x/C$ samples increased by ~3.5 times.

In addition to the significantly enhanced ORR activity, $AuPt_x/C$ catalysts also showed excellent durability under the oxidizing potentials in acid media. Taking $AuPt_{0.38}/C$ and $AuPt_{0.58}/C$ catalysts, for example, Figure 7 shows CVs and ORR polarization curves before and after the catalysts were subject to accelerated electrochemical degradation tests of repeating potential cycling between 0.6 and 1.1 V in 0.1 M $HClO_4$ saturated with O_2, which mimics the cathode working conditions of PEMFCs. After 10 000 cycles, the ECSA of Pt, indicated by the hydrogen adsorption/desorption current in potential region below 0.4 V and the reduction current in potential region between 0.9 and 0.5 V, decreased slightly (Figure 7a,c). This may be due to dissolution and/or aggregation of surface Pt atoms. It is also possible that some small amount of surface Pt atoms diffused into interior of particle due to the relatively larger surface energy of Pt than that of Au. As shown in Figure 7b,d, the ORR polarization curves show negligible change after 10 000 cycles of potential cycling, indicating that the ORR activity of $AuPt_x/C$ catalysts can sustain during long-term use in working conditions of PEMFCs cathode. In comparison, Pt/C showed significant loss in ECSA and ORR activity under similar treatment.[20]

4. CONCLUSIONS

We have shown through TEM, XPS, EDS, and electrochemical measurements that Pt can be spontaneously deposited on the surface of Au nanoparticles in solution containing $PtCl_4^{2-}$, without adding any extraneous reducing agents and performing any chemical or electrochemical pre/post-treatments of Au surface. The spontaneous deposition yields uniformly distributed Pt atoms on the surface of Au nanoparticles, without formation of islands or dendritic branches. Significant deposition of Pt occurs only as the concentration of $PtCl_4^{2-}$ is above ca. 10^{-4} mol/L. The coverage of Pt increases significantly with the deposition temperature. Approximately a monolayer of Pt can be formed at temperature of ca. 80 °C. The resulting nanoparticles of Pt on Au have significantly enhanced electrocatalytic activity for the ORR as compared with pure Pt nanoparticles, with the specific and mass activity of Pt increasing by ca. 3.5 times. More importantly, these nanoparticle catalysts exhibit excellent durability under oxidizing potentials in acid media, in contrast to the relatively poor stability of pure Pt nanoparticle catalyst. The present one-step spontaneous deposition of Pt on Au should represent a straightforward approach for scale-up production of ORR electrocatalyst for PEMFCs.

AUTHOR INFORMATION

Corresponding Author

*E-mail: slchen@whu.edu.cn.

Notes

The authors declare no competing financial interest.

ACKNOWLEDGMENTS

This work is supported by the Ministry of Science and Technology (Grant Nos. 2012CB932800 and 2013AA110201), the National Natural Science Foundation of China (Grant No. 21073137), and the Fundamental Research Founds for National University (CUG120803), China University of Geosciences (Wuhan).

REFERENCES

(1) Gasteiger, H. A.; Markovic, N. M. Just a Dream-or Future Reality? *Science* **2009**, *324*, 48−49.

(2) Debe, M. K. Electrocatalyst Approaches and Challenges for Automotive Fuel Cells. *Nature* **2012**, *486*, 43−51.

(3) Stamenkovic, V.; Mun, B. S.; Mayrhofer, K. J. J.; Ross, P. N.; Markovic, N. M.; Rossmeisl, J.; Greeley, J.; Norskov, J. K. Changing the Activity of Electrocatalysts for Oxygen Reduction by Tuning the Surface Electronic Structure. *Angew. Chem., Int. Ed.* **2006**, *45*, 2897−2901.

(4) Shao, M. H.; Peles, A.; Shoemaker, K.; Gummalla, M.; Njoki, P. N.; Luo, J.; Zhong, C. J. Enhanced Oxygen Reduction Activity of Platinum Monolayer on Gold Nanoparticles. *J. Phys. Chem. Lett.* **2011**, *2*, 67−72.

(5) Fennell, J.; He, D. S.; Tanyi, A. M.; Logsdial, A. J.; Johnston, R. L.; Li, Z. Y.; Horswell, S. L. A Selective Blocking Method to Control the Overgrowth of Pt on Au Nanorods. *J. Am. Chem. Soc.* **2013**, *135*, 6554−6561.

(6) Hartl, K.; Mayrhofer, K. J. J.; Lopez, M.; Goia, D.; Arenz, M. AuPt Core-Shell Nanocatalysts with Bulk Pt Activity. *Electrochem. Commun.* **2010**, *12*, 1487−1489.

(7) Cheng, S.; Rettew, R. E.; Sauerbrey, M.; Alamgir, F. M. Architecture-Dependent Surface Chemistry for Pt Monolayers on Carbon-Supported Au. *ACS Appl. Mater. Interfaces* **2011**, *3*, 3948−3956.

(8) Nutariya, J.; Fayette, M.; Dimitrov, N.; Vasiljevic, N. Growth of Pt by Surface Limited Redox Replacement of Underpotentially Deposited Hydrogen. *Electrochim. Acta* **2013**, *112*, 813−823.

(9) Crown, A.; Johnston, C.; Wieckowski, A. Growth of Ruthenium Islands on Pt(*hkl*) Electrodes Obtained via Repetitive Spontaneous Deposition. *Surf. Sci.* **2002**, *506*, L268−L274.

(10) Patra, S.; Das, J.; Yang, H. Selective Deposition of Pt on Au Nanoparticles Using Hydrogen Presorbed into Au Nanoparticles during $NaBH_4$ Treatment. *Electrochim. Acta* **2009**, *54*, 3441−3445.

DOI: 10.1021/am5073029
ACS Appl. Mater. Interfaces 2015, 7, 823−829

(11) Du, B. C.; Tong, Y. Y. A Coverage-Dependent Study of Pt Spontaneously Deposited onto Au and Ru Surfaces: Direct Experimental Evidence of the Ensemble Effect for Methanol Electro-Oxidation on Pt. *J. Phys. Chem. B* **2005**, *109*, 17775−17780.
(12) Bakos, I.; Szabó, S.; Pajkossy, T. Deposition of Platinum Monolayers on Gold. *J. Solid State Electrochem.* **2011**, *15*, 2453−2459.
(13) Nagahara, Y.; Hara, M.; Yoshimoto, S.; Inukai, J.; Yau, S. L.; Itaya, K. In Situ Scanning Tunneling Microscopy Examination of Molecular Adlayers of Haloplatinate Complexes and Electrochemically Produced Platinum Nanoparticles on Au(111). *J. Phys. Chem. B* **2004**, *108*, 3224−3230.
(14) Kim, S.; Jung, C.; Kim, J.; Rhee, C. K.; Choi, S. M.; Lim, T. H. Modification of Au Nanoparticles Dispersed on Carbon Support Using Spontaneous Deposition of Pt toward Formic Acid Oxidation. *Langmuir* **2010**, *26*, 4497−4505.
(15) Zheng, F. L.; Wong, W. T.; Yung, K. F. Facile Design of Au@Pt Core−Shell Nanostructures: Formation of Pt Submonolayers with Tunable Coverage and Their Applications in Electrocatalysis. *Nano Res.* **2014**, *7*, 410−417.
(16) Strbac, S.; Petrovic, S.; Vasilic, R.; Kovac, J.; Zalar, A.; Rakocevic, Z. Carbon Monoxide Oxidation on Au(111) Surface Decorated by Spontaneously Deposited Pt. *Electrochim. Acta* **2007**, *53*, 998−1005.
(17) Brankovic, S. R.; Marinkovic, N. S.; Wang, J. X.; Adzic, R. R. Carbon Monoxide Oxidation on Bare and Pt-Modified Ru(1010) and Ru(0001) Single Crystal Electrodes. *J. Electroanal. Chem.* **2002**, *532*, 57−66.
(18) Brankovic, S. R.; McBreen, J.; Adzic, R. R. Spontaneous Deposition of Pt on the Ru(0001) Surface. *J. Electroanal. Chem.* **2001**, *503*, 99−104.
(19) Brankovic, S. R.; Marinkovic, N. S.; Wang, J. X.; Adzic, R. R. Electrosorption and Catalytic Properties of Bare and Pt Modified Single Crystal and Nanostructured Ru Surfaces. *J. Electroanal. Chem.* **2002**, *524−525*, 231−241.
(20) Dai, Y.; Ou, L. H.; Liang, W.; Yang, F.; Liu, Y. W.; Chen, S. L. Efficient and Superiorly Durable Pt-Lean Electrocatalysts of Pt-W Alloys for the Oxygen Reduction Reaction. *J. Phys. Chem. C* **2011**, *115*, 2162−2168.

DOI: 10.1021/am5073029
ACS Appl. Mater. Interfaces 2015, 7, 823−829